TÜBİTAK

Turkish Journal of Veterinary and Animal Sciences

http://journals.tubitak.gov.tr/veterinary/

Research Article

Turk J Vet Anim Sci
(2014) 38: 363-369

doi:10.3906/vet-1401-44

Immunohistochemical localization of glutathione peroxidase 1 enzyme and its gene expression by RT-PCR in the liver tissue of healthy and diabetic mice

Turgay DEPREM*, Nurhayat GÜLMEZ
Department of Histology and Embryology, Faculty of Veterinary Medicine, Kafkas University, Kars, Turkey

Received: 13.01.2014 • **Accepted:** 24.03.2014 • **Published Online:** 17.06.2014 • **Printed:** 16.07.2014

Abstract: The purpose of this study is to examine the gene expression level of glutathione peroxidase 1 (GPx1) in the liver of healthy and diabetic mice, its localization in the tissue, and structural changes in the liver. In this study, 36 Swiss albino mice were divided into 3 groups: experimental (diabetic) (n = 15), sham (n = 15), and control (n = 6). Streptozotocin (100 mg/kg) was intraperitoneally administered to mice in the experimental group. While the gene expression level of GPx1 was determined using the RT-PCR method, its localization in the liver was determined using an immunohistochemical method. The GPx1 enzyme activity of the experimental group was lower compared to the sham and control groups ($P < 0.05$). There was no difference between the experimental and sham groups in terms of the gene expression of GPx1; however, a statistically insignificant decrease was observed in the experimental group compared to the sham group. GPx1 had similar immunolocalization in all groups, but GPx1 immunoreactivity was lower in the experimental group compared to the other groups. Enlargement of hepatocytes and their nuclei as well as the presence of intranuclear inclusion bodies were observed in the experimental group. In conclusion, diabetes mellitus causes a decrease in the level of GPx1 activity, which is known to be one of the antioxidant enzymes.

Key words: Diabetes mellitus, liver, GPx1, RT-PCR, immunohistochemistry

1. Introduction

Being a result of problems of insulin production and use in the body, diabetes mellitus is a disease associated with total or partial insulin deficiency and characterized by hyperglycemia (1). The formation rate of free radicals in organisms and their removal rate should be in balance (oxidative balance). Changing the delicate balance between free radicals and the antioxidant defense system to prooxidant and oxidant substances causes the development of oxidative stress. It has been shown that oxidative stress causes tissue damage, and it is a factor in the development of pathological status such as cancer, diabetes, and atherosclerosis (2). Glutathione peroxidase (GPx; EC 1.11.1.9), which is one of the natural antioxidant defense systems against free radicals, catalyzes the reduction of hydrogen peroxide (H_2O_2) or organic hydroperoxides into water or alcohols by using reduced glutathione (3). In this manner, it prevents lipid peroxidation and thus protects cell membranes from oxidative damage (4). The distribution of glutathione peroxidase is wide in the tissues of mammals and the liver is one of the richest sources (5). Type I diabetes can be triggered for experimental purposes via a commonly used streptozotocin (STZ) injection in order to examine the complications caused by diabetes and determine treatment approaches (6). It is known that free fatty acids and various free radical-derived antioxidants show an increase in diabetes and this increase causes numerous systemic disorders (7). A decrease in the quantity of antioxidant parameters in diabetics, such as vitamins C and E, glutathione, SOD, CAT, and GPx, shows that oxidative stress can have a significant role in the pathogenesis of chronic complications of diabetes (8). The purpose of this study was to examine the gene expression level of glutathione peroxidase 1 (GPx1) in the livers of healthy and diabetic (Type I) mice, the localization of enzyme in the tissue, and structural changes in the liver.

2. Materials and methods

The experimental applications performed on mice were carried out with approval from the Kafkas University Animal Experiments Local Ethics Committee (04.04.2007/13).

Thirty-six 8- to 12-week-old male Swiss albino mice were used. Mice used in the experiment were divided into 3 groups as experimental (diabetic) (n = 15), sham (n = 15), and control (n = 6). A single dose of 100 mg/kg (9) STZ (Sigma, St Louis, MO, USA) dissolved in 0.1 M fresh citrate buffer (pH 4.5) was intraperitoneally administered to

* Correspondence: turgaydeprem@hotmail.com

the mice in the experimental group and 0.1 M citrate buffer alone was administered to the sham group. No application was performed on the mice in the control group. The start-time of the experiment was labeled as "0", and the body weights of mice were measured after 8 h of hunger on days 0, 3, 7, 15, 21, and 30. Afterwards, blood glucose values were determined using a manual glucose meter (Accu-Chek-Go, Roche, Basel, Switzerland) in blood taken from the orbital sinuses using a hematocrit tube. Blood glucose values after 8 h of hunger were measured 72 h after STZ administration, and mice having values of 200 mg/dL and above were accepted as diabetic (9) and included in the study.

Liver tissue samples were taken by euthanizing mice with cervical dislocation under ether anesthesia on days 3, 15, and 30. The liver tissue taken for molecular analysis was homogenized in Tri-Reagent (Sigma) and kept at 4 °C until the day of analysis. Liver tissue samples allocated for histological and immunohistochemical analyses were fixed in Bouin and formol-alcohol solutions.

Some liver tissue samples were blocked in paraffin after routine tissue follow-up and 6-µm-thick sections were taken. Crossman's triple staining, hematoxylin-eosin staining, and periodic acid–Schiff staining were applied. The avidin-biotin-peroxidase complex technique was performed in order to investigate the immunohistochemical distribution of GPx1 in the liver tissue. The sections were incubated with anti-GPx1 (Abcam-ab22604) (1:3000) at room temperature for 1 h. After irrigation with phosphate buffered saline (PBS), the biotinylated secondary antibody (Ultravision Detection System Anti-Rabbit, Biotinylated Goat Anti-Rabbit, LabVision-510.991.2800), against the type for which the primary antibody is produced, was applied to sections for 30 min. Then, after further irrigation with PBS, streptavidin-horse radish peroxidase was added to the sections and kept at room temperature for 30 min. After irrigation with PBS again, the DAB-H_2O_2 technique was used for chromogen application. The preparations were examined using a BX-051 Olympus microscope and their photographs were taken.

GPx enzyme activity was measured according to the method of Matkovics et al. (10). Total RNA isolation, obtained as a result of modification of the guanidine isothiocyanate/phenol-chloroform method described by Chomczynski and Sacci (11), was carried out using Tri-Reagent (Sigma). The amount of RNA per microliter was measured using a spectrophotometer at 260 nm wavelength. mRNAs were obtained using Oligo dT primers (Promega, Madison, WI, USA). An MMLV RT master mixture was prepared in order to obtain cDNA (Moloney Murine Leukemia Virus Reverse Transcriptase). For each sample, 8 µL of MMLV enzyme buffer, 8 µL of dNTP (Sigma), 1 µL of rRNAsin (Promega), 1.6 µL of MMLV-RT enzyme (Promega), and 6.4 µL of NF water, at 25 µL in total, was used. Once 25 µL of the master mixture was added into each of the tubes containing mRNA marked with oligo DT, the tubes were kept in the PCR device at 37 °C for 1 h, at 95 °C for 5 min, and at 4 °C for 5 min in order to obtain cDNA. Regarding DNA multiplication, 50 µL of master mixture (5 µL of Taq buffer, 1 µL of dNTP, 1 µL of forward primer, 1 µL of reverse primer, 1 µL of enzyme Taq (Sigma), and 41 µL of nuclease-free water) was added to each tube containing 2 µL of cDNA and the tubes were processed in the PCR device at 94 °C for 5 min, at 50 °C for 1 min, and at 72 °C for 1.5 min (24 cycles for GPx1 and 30 cycles for β-actin). While the forward primer was 5'-CCT CAA GTA CGT CCG ACC TG-3' and the reverse was 5'-CAA TGT CGT TGC GGC ACA CC-3' (12) in primer sequences for the GPx1 gene, for β-actin, the forward was 5'-TCA TGA AGT GTG ACG TTG ACA TCC GT-3' and the reverse was 5'-CCT AGA AGC ATT TGC GGT GCA CGA TG-3' (13). The end products of the RT-PCR were processed in a gel electrophoresis device at 100 V for 1 h with a 1.5% agarose gel. The resulting gel products were assessed by taking their photographs under UV light. Band densitometries for β-actin and GPx1 in the gel products were obtained using the Kodak ID program. The densitometric data of GPx1 were then normalized and statistically analyzed with reference to β-actin.

SPSS 12.0 was used to conduct the statistical analysis. Possible differences were determined using Student's t-test and analysis of variance. The confidence interval was set at 0.05 for the statistical analysis.

3. Results

It was observed that the mean body weights of the experimental group decreased daily ($P < 0.05$). Liver weight was statistically higher in all days in the experimental group compared to the sham and control groups ($P < 0.05$; Figure 1). Subsequently, depending on time, a regular increase was observed in liver weight in the experimental group ($P < 0.05$). It was determined that the experimental

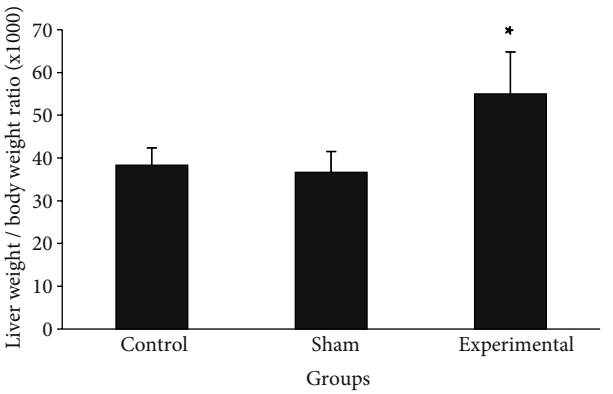

Figure 1. Comparison of liver weights between groups (* = $P < 0.05$).

group had lower GPx1 enzyme activity in the liver tissue compared to the sham and control groups ($P < 0.05$).

The livers of mice in the sham and control groups were observed to have normal histological structure (Figure 2A). On day 3, the outer surfaces of some cell nuclei became irregular in the liver tissue of the experimental group, and lesions like swelling were found in the nuclei. A significant enlargement (megalocytosis) was observed in the hepatocytes and nuclei of the mice livers in the experimental group on day 15 compared to day 3. Cell nuclei also became irregular during this period (Figure 2B). In contrast to the lesions identified on day 3, cytoplasmic invaginations with eosinophilic character and globular structure in the nucleus were encountered on day 15 (Figure 2B). Histological findings of the liver sections of the experimental group on day 30 were similar to those obtained on day 15 (Figure 2C).

GPx1 immunoreactivity was observed in all of the groups: sham, control, and diabetic. On day 3 of the experiment, periacinar staining was seen in all of the groups. The staining was present variably in both nuclei and cytoplasm (Figure 3A). The staining in the hepatocytes located around the Kiernan space was more intense compared to those located in the periacinar regions (Figure 3B). Staining characteristics for all the treatment days/groups were similar to each other and some cells showed cytoplasmic and/or nuclear staining throughout the sections (Figure 3C). Moreover, GPx1 immunoreactivity in the diabetic group (Figure 4A) was lower compared to the sham group on day 15 (Figure 4B). GPx1 immunoreactivity findings in the liver on day 30 were similar to those obtained on days 3 and 15.

No statistically significant difference was observed between the experimental and sham groups in terms of β-actin (control) gene expression in the liver tissue (Figure 5A). Even though there was no statistical difference between the sham and diabetic groups in terms of GPx1 gene expression on day 3, GPx1 gene expression was higher at a statistically insignificant level in the diabetic group on day 3; however, although there was no statistical difference in the diabetic group in terms of GPx1 gene expression between days 15 and 30, GPx1 gene expression decreased at a statistically insignificant level in the diabetic group (Table; Figure 5B). The experimental group also had a statistically insignificant decrease in GPx1 gene expression over the time period of the study (Table).

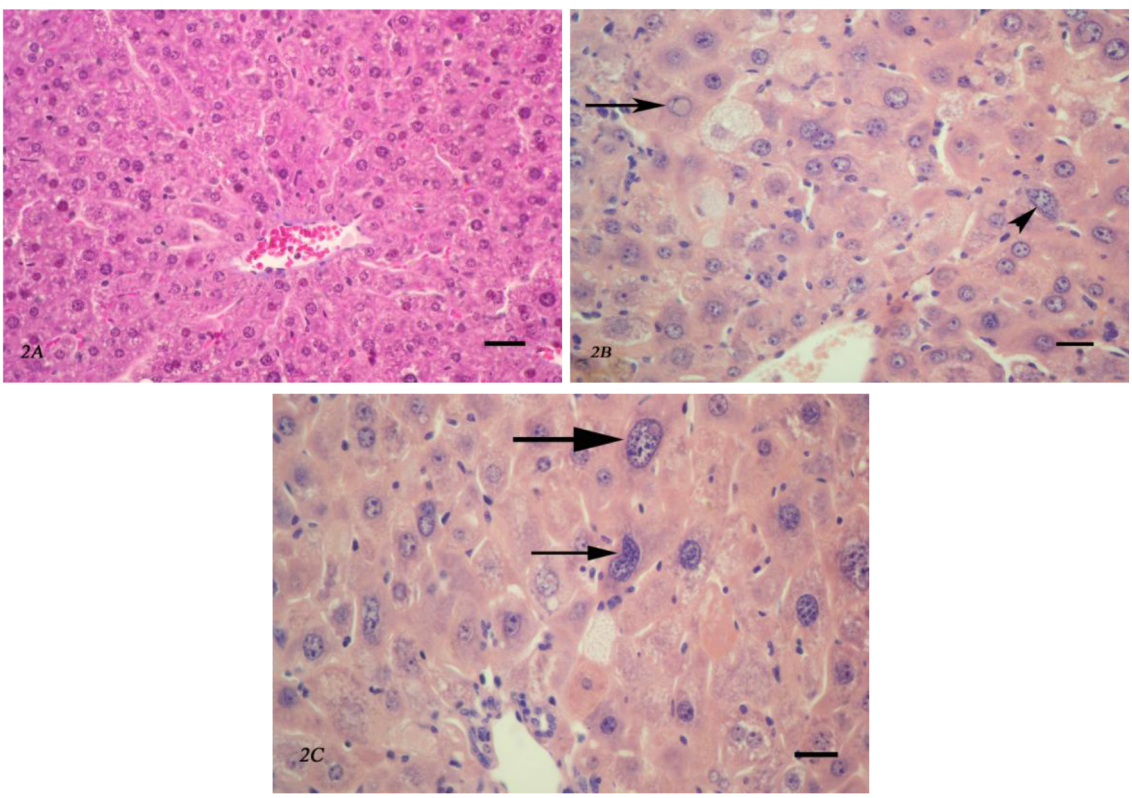

Figure 2. A) Histological view of livers of mice in the control group, with triple staining. Bar = 50 µm. **B)** Histological view of livers of diabetic mice on day 15. Arrow head = nuclei of impaired hepatocyte, thin arrow = spherical or oval eosinophilic inclusion bodies in nucleus, bar = 50 µm. **C)** Histological view of livers of diabetic mice on day 30. Thick arrow = megalocytosis in hepatocytes, thin arrow = impaired nuclei of hepatocytes, and bar = 50 µm.

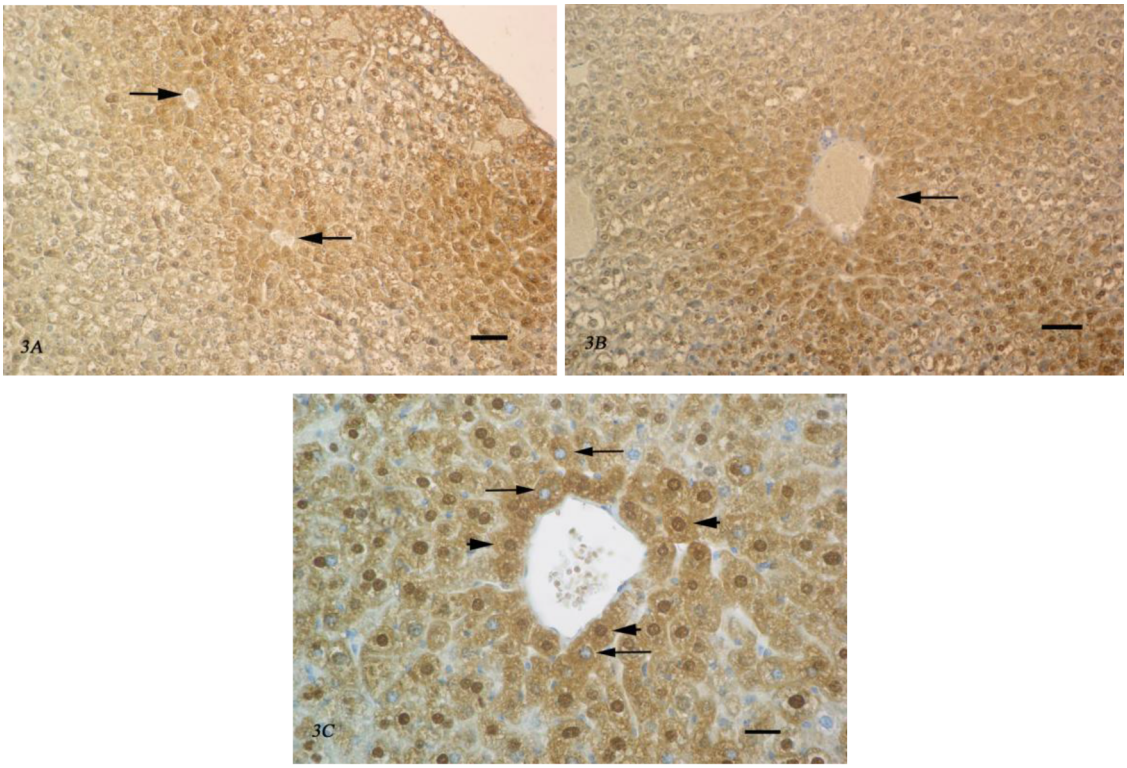

Figure 3. A) Intense GPx1 immunoreactivity in the periacinar hepatocytes in the experimental group on day 3. Arrows = vena centralis, bar = 100 µm. **B)** Intense GPx1 immunoreactivity in hepatocytes around the Kiernan space of livers of mice in the experimental group on day 3. Arrow = hepatocytes, bar = 100 µm. **C)** Cytoplasmic and nuclear GPx1 immunoreactivity in hepatocytes of mouse livers in the sham group on day 15. Arrows = cytoplasmic GPx1 immunoreactivity, arrow head = cytoplasmic and nuclear GPx1 immunoreactivity, bar = 50 µm.

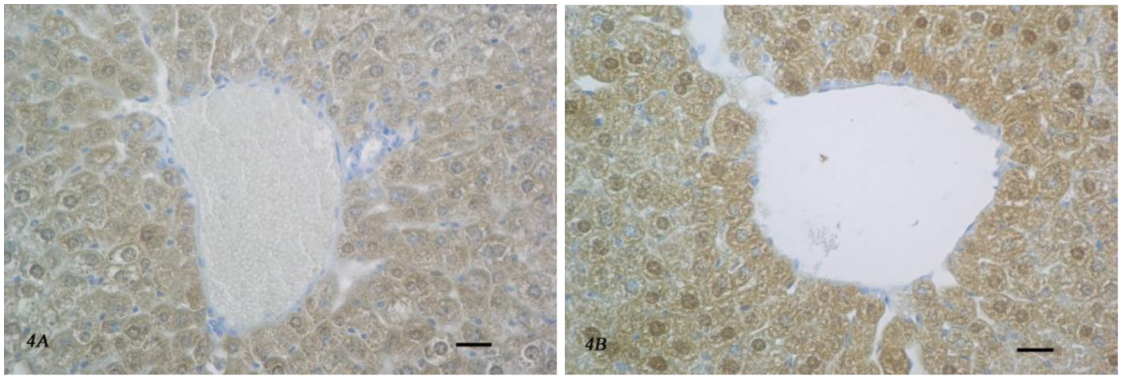

Figure 4. A) GPx1 immunoreactivity in the livers of mice in the experimental group on day 15. **B)** GPx1 immunoreactivity in the livers of mice in the sham group on day 15. Bar = 50 µm.

4. Discussion

Studies conducted on body weight changes in diabetes (14–17) revealed different results. Watkins et al. (17) reported that there was no difference between the control and diabetic groups during a period of 42 days in terms of the mean body weight of mice. Fujita et al. (15) stated a significant decrease in the body weight in STZ diabetic mice compared to the control. Doi et al. (14) stated that the body weight of diabetic mice decreased compared to the control mice at the end of a 4-week-long period, and the body weights of the STZ group increased during the study period. Imaeda et al. (16) indicated that there was a decrease in the body weights of mice under STZ administration, especially on day 7. This study revealed a

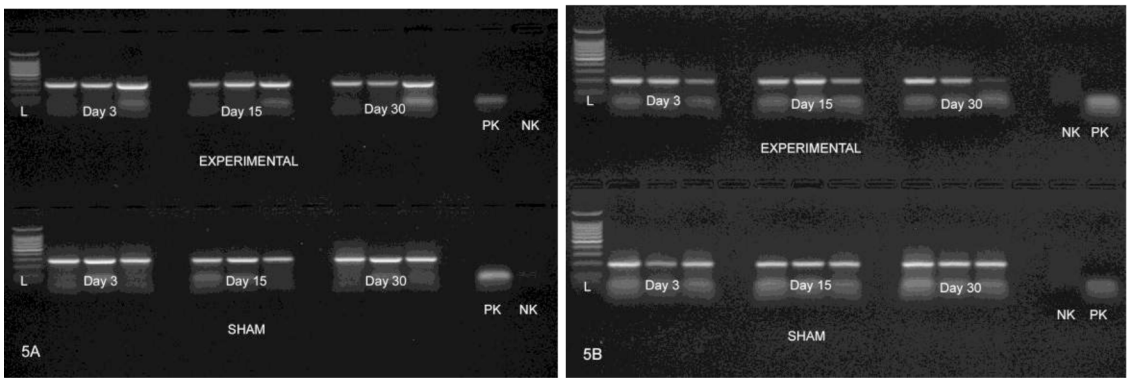

Figure 5. A) β-Actin gene RT-PCR results (product size: 285 base pairs). **B)** GPx1 gene RT-PCR results (product size: 197 base pairs). PK = positive control, NK = negative control, L = 100-bp DNA ladder.

Table. Comparison of mean GPx1 gene expression levels of groups by day.

GPx1 gene expression levels (arbitrary units)										
Group	Number (n)	Day 3			Day 15			Day 30		
		Mean rank	SD	F-value	Mean rank	SD	F-value	Mean rank	SD	F-value
Experimental	3	0.80	0.49	0.16^{ns}	0.82	0.42	0.11^{ns}	0.65	0.51	0.02^{ns}
Sham	3	0.67	0.23		0.91	0.21		0.69	0.06	

SD = Standard deviation, ns = not significant.

decrease in the mean body weight of STZ diabetic mice during the 4-week-long experimental period, and the fact that this loss of body weight became evident on day 7 shows a parallelism with the findings of Imaeda et al. (16). Researchers (18) stated that weight loss in diabetes was observed during the lipolysis and gluconeogenesis processes occurring while cells obtain glucose.

Reports stated that experimental diabetes increased (14,19), decreased (18), or did not change (17) liver weight. We determined in this study that liver weight increased in the diabetic group compared to the sham and control groups, and the liver weight of the diabetic group increased during the period, as well. Our results are parallel to the results of Cho et al. (19) and Doi et al. (14).

While Garg et al. (20) reported an increase in GPx enzyme activity in the diabetic liver compared to the control and Can et al. (21) reported a decrease in GPx enzyme activity in the diabetic liver, Kinalski et al. (22) found no difference. In this study, we determined that GPx activity in STZ diabetic mice was lower compared to the control and sham groups, which supported the results of researchers stating that enzyme activity decreased (19,21). As reported by Bonnefont-Rousselot et al. (23), it was thought that the decrease in GPx level could be associated with the fact that antioxidant enzymes became inactive as a result of glycosylation due to hyperglycemia in diabetes.

In their 4-week-long and 6-week-long studies, Otsuka et al. (24) determined using the RT-PCR method that GPx mRNA level considerably decreased in the livers of diabetic rats compared to control rats. Cho et al. (19) examined hepatic antioxidant enzyme activities and lipid profiles of diabetic rats via northern blot analysis and reported that hepatic GPx mRNA concentrations in the diabetic group slightly decreased compared to the control even though this was not statistically significant. This study revealed that although there was no statistical difference between the sham group and the diabetic group on day 3, the concentration was higher in the diabetic group. However, it decreased in the diabetic group even though there was no statistical difference on days 15 and 30. Results obtained on days 15 and 30 show parallelism with those of the study conducted by Cho et al. (19). A statistically insignificant decrease was determined in GPx1 gene expression in the experimental group on day 30 compared to days 3 and 15 in this study. The reason for this statistically insignificant decrease was thought to be associated with the period.

Watkins et al. (17), who examined the livers of STZ diabetic mice at the electron microscopic level, reported

swelling in the hepatic sinuses, especially on the first and third days, and a visible enlargement between hepatocyte boundaries. While some researchers developing diabetes in mice using STZ (14,25) noted that the hepatocyte nucleus area increased, some (25,26) reported that the size of the cell increased (hypertrophy). Honjo et al. (26) revealed that cytoplasmic invaginations formed in the hepatocyte nucleus. Doi et al. (14) reported that the hepatocyte nucleus area in STZ diabetic mice was nearly twice as large as the controls and showed irregular structures. Can et al. (21) stated that the liver cellular layers of diabetic rats became impaired due to degeneration of hepatocytes, most liver cells seemed vacuolated, and swollen hepatocytes included eosinophilic intracytoplasmic inclusions. In this study, it was observed that the cell took the shape of a signet ring by pushing aside nuclei of some liver hepatocytes in the diabetic group. The outer sides of these cell nuclei became irregular, and swelling-like lesions were also found in the nuclei. The fact that an enlargement (megalocytosis) was observed in hepatocytes and their nuclei in the livers of the experimental group on day 15 compared to day 3 was in line with the results of Laguens et al. (25) and Doi et al. (14). Unlike the lesions detected on day 3, cytoplasmic invaginations with intranuclear eosinophilic character and globular structure were frequently found, which is in line with the data of Can et al. (21).

Yoshimura et al. (27) reported that in terms of immunohistochemistry, GPx was diffusely localized in the cytoplasm of hepatocytes in the livers of rats, a stronger staining occurred in the periphery of the hepatic lobe compared to the central zone around the central vein, and endothelial cells around the sinusoids and Kupffer cells were not stained. Asayama et al. (28) indicated that cellular GPx was found in the cytoplasm, nuclei, mitochondria, and other organelles of the hepatocytes of rats using the immunogold technique. Asayama et al. (29) stated that GPx1 was immunohistochemically stained with a similar concentration in the centrilobular area and periphery around the central vein in the liver hepatocyte cells of fetal and neonatal rats. Utsunomiya et al. (30) explained in their study that the immunoreactivity of GPx was stronger especially in the cytosol of hepatocytes in the periportal zone, and GPx gave a positive reaction in both the cytoplasm and nuclei of hepatocytes. In a study (27) conducted using immunoelectron microscopy, GPx was observed to be intensely localized in the cytoplasm of the periportal hepatocytes in rat liver. After a literature review, it was determined that there was no information about the immunoreactivity of GPx1 in diabetes; GPx1 showed similar immunolocalization in the livers of the control, sham, and diabetic groups in this study, and GPx1 immunoreactivity in the diabetic group was lower compared to the sham group. GPx1 immunoreactivity, which showed diffuse cytoplasmic and/or nuclear staining, was generally similar in our study to that reported by Asayama et al. (29).

GPx1 immunoreactivity was observed to be more intense in hepatocytes around the vena centralis and Kiernan space. However, GPx1 immunoreactivity was not observed in vein endothelial cells of the vena centralis and the endothelial and connective tissue of veins in the Kiernan space. Our results support the data of Yoshimura et al. (27).

In conclusion, it was observed that diabetes mellitus caused a significant decrease in the tissue activity in the GPx gene expression in the liver that is not reflected by the statistics. We are of the opinion that the results obtained in our study may vary according to the period of the experiment, species of the experimental animals used, and individual differences. We suggest that the results of this study will shed light for new studies to be conducted via advanced techniques in order to clarify the relationship between diabetes mellitus and antioxidants.

Acknowledgments

This study was supported by the Kafkas University Scientific and Technological Research Fund (Project No: 2007-VF-014). It was summarized from a doctoral dissertation and was also presented at the 11th National Histology and Embryology Congress, 16–19 May 2012, Denizli, Turkey.

References

1. Abou-Seif MA, Youssef AA. Evaluation of some biochemical changes in diabetic patients. Clin Chim Acta 2004; 346: 161–170.
2. Cross CE, Halliwell B, Borish ET, Pryor WA, Ames BN, Saul RL, McCord JM, Harman D. Oxygen radicals and human disease. Ann Intern Med 1987; 107: 526–545.
3. Herbette S, Roeckel-Drevet P, Drevet JR. Seleno-independent glutathione peroxidases. More than simple antioxidant scavengers. FEBS J 2007; 274: 2163–2180.
4. Czuczejko J, Zachara BA, Staubach-Topczewska E, Halota W, Kedziora J. Selenium, glutathione and glutathione peroxidases in blood of patients with chronic liver diseases. Acta Biochim Pol 2003; 50: 1147–1154.
5. Stadtman TC. Biological function of selenium. Nutr Rev 1977; 35: 161–166.
6. Sanai T, Sobka T, Johnson T, el-Essawy M, Muchaneta-Kubara EC, Ben Gharbia O, el Oldroyd S, Nahas AM. Expression of cytoskeletal proteins during the course of experimental diabetic nephropathy. Diabetologia 2000; 43: 91–100.

7. Scott JS, King GL. Oxidative stress and antioxidant treatment in diabetes. Ann NY Acad Sci 2004; 1031: 204–213.

8. Lipinski B. Pathophysiology of oxidative stress in diabetes mellitus. J Diabetes Complications 2001; 15: 203–210.

9. Kanitkar M, Bhonde R. Existence of islet regenerating factors within the pancreas. Rev Diabet Stud 2004; 1: 185–192.

10. Matkovics B, Szabo L, Varga I. Determination of enzyme activities in lipid peroxidation and glutathione pathways. Lab Diag 1988; 15: 248–250.

11. Chomczynski P, Sacchi N. Single-step method of RNA isolation by acid guanidinium thiocyanate-phenol-chloroform extraction. Anal Biochem 1987; 162: 156–159.

12. Ferret PJ, Soum E, Negre O, Fradelizi D. Auto-protective redox buffering systems in stimulated macrophages. BMC Immunol 2002; 12: 3.

13. Kocamış H. Functional profiles of growth related genes during embryogenesis and postnatal development of chicken and mouse skeletal muscle. PhD, West Virginia University, Morgantown, WV, USA, 2001.

14. Doi K, Yamanouchi J, Kume E, Yasoshima A. Morphologic changes in hepatocyte nuclei of streptozotocin (SZ)-induced diabetic mice. Exp Toxicol Pathol 1997; 49: 295–299.

15. Fujita A, Sasaki H, Ogawa K, Okamoto K, Matsuno S, Matsumoto E, Furuta H, Nishi M, Nakao T, Tsuno T et al. Increased gene expression of antioxidant enzymes in KKAy diabetic mice but not in STZ diabetic mice. Diabetes Res Clin Pract 2005; 69: 113–119.

16. Imaeda A, Kaneko T, Aoki T, Kondo Y, Nagase H. DNA damage and the effect of antioxidants in streptozotocin-treated mice. Food Chem Toxicol 2002; 40: 979–987.

17. Watkins JB 3rd, Gardner PA, Feczko JD, Klueber KM. Streptozotocin and insulin-dependent diabetes induce changes in hepatic cytoarchitecture in mice. Int J Toxicol 2000; 19: 401–405.

18. Noorafshan A, Esmail-Zadeh B, Bahmanpour S, Poost-Pasand A. Early stereological changes in liver of Sprague-Dawley rats after streptozotocin injection. Indian J Gastroenterol 2005; 24: 104–107.

19. Cho SY, Park JY, Park EM, Choi MS, Lee MK, Jeon SM, Jang MK, Kim MJ, Park YB. Alternation of hepatic antioxidant enzyme activities and lipid profile in streptozotocin-induced diabetic rats by supplementation of dandelion water extract. Clin Chim Acta 2002; 317: 109–117.

20. Garg MC, Bansal DD. Protective antioxidant effect of vitamins C and E in streptozotocin induced diabetic rats. Indian J Exp Biol 2000; 38: 101–104.

21. Can B, Ulusu NN, Kilinç K, Acan NL, Saran Y, Turan B. Selenium treatment protects diabetes-induced biochemical and ultrastructural alterations in liver tissue. Biol Trace Elem Res 2005; 105: 135–150.

22. Kinalski M, Sledziewski A, Telejko B, Zarzycki W, Kinalska I. Lipid peroxidation and scavenging enzyme activity in streptozotocin-induced diabetes. Acta Diabetol 2000; 37: 179–183.

23. Bonnefont-Rousselot D, Bastard JP, Jaudon MC, Delattre J. Consequences of the diabetic status on the oxidant/antioxidant balance. Diabetes Metab 2000; 26: 163–176.

24. Otsuka Y, Ueta E, Yamamoto T, Tadokoro Y, Suzuki E, Nanba E, Kurata T. Effect of streptozotocin-induced diabetes on rat liver mRNA level of antioxidant enzymes. Int Cong Ser 2002; 1245: 421–423.

25. Laguens RP, Candela S, Hernández RE, Gagliardino JJ. Streptozotocin-induced liver damage in mice. Horm Metab Res 1980; 12: 197–201.

26. Honjo K, Doi K, Doi C, Mitsuoka T. Histopathology of streptozotocin-induced diabetic DBA/2N and CD-1 mice. Lab Anim 1986; 20: 298–303.

27. Yoshimura S, Komatsu N, Watanabe K. Purification and immunohistochemical localization of rat liver glutathione peroxidase. Biochem Biophsy Acta 1980; 621: 130–137.

28. Asayama K, Yokota S, Dobashi K, Hayashibe H, Kawaoi A, Nakazawa S. Purification and immunoelectron microscopic localization of cellular glutathione peroxidase in rat hepatocytes: quantitative analysis by postembedding method. Histochemistry 1994; 102: 213–219.

29. Asayama K, Dobashi K, Kawada Y, Nakane T, Kawaoi A, Nakazawa S. Immunohistochemical localization and quantitative analysis of cellular glutathione peroxidase in foetal and neonatal rat tissues: fluorescence microscopy image analysis. Histochem J 1996; 28: 63–71.

30. Utsunomiya H, Komatsu N, Yoshimura S, Tsutsumi Y, Watanabe K. Exact ultrastructural localization of glutathione peroxidase in normal rat hepatocytes: advantages of microwave fixation. J Histochem Cytochem 1991; 39: 1167–1174.